

**Framework Programme (FP) 7
Clean Sky Joint Undertaking
SP1-Cooperation**

SP1-JTI-CS-2010-03-271882

FATIMA

Fatigue testing of CFRP materials

Final Report



Project Coordinator	Dr. Jürgen Keller AMIC Angewandte Micro-Messtechnik GmbH		
Start date Project	1 Januar 2011	Duration	36 months
Version	1.0		
Status	Final		
Date of issue	27. Feb. 2014		
Filename	2014_02_27_FinalReport_FATIMA.doc		

0 DOCUMENT INFO

0.1 AUTHORS

Author	Company	e-mail
Jürgen Keller	AMIC	Juergen.Keller@amic-berlin.de
Bettina Seiler	CWM	seiler@cwm-chemnitz.de
Thomas Winkler	Nanotest	Thomas.Winkler@nanotest.org

0.2 DOCUMENT KEYDATA

Keywords	SP1-JTI-CS-2010-03-271882-FATIMA, Final Report	
Editor Address data	Name	Jürgen Keller
	Coordinator	AMIC Angewandte Micro-Messtechnik GmbH
	Address	Volmerstrasse 9B, 12489 Berlin
	Phone	+49 30 6392 2540
	E-mail :	Juergen.Keller@amic-berlin.de

0.3 DISTRIBUTION LIST

Date	Issue
27/02/2014	Report to EC – Project Officer

© FATIMA Consortium

This document will be treated strictly confidential within the consortium.

Table of Contents

Executive Summary	4
Summary description of project context and objectives	5
Description of main S & T results/foregrounds	8
1 WP Humidity Expansion	8
1.1 Methodology	8
1.2 Experimental Procedure	9
1.2.1 Results – Material: HexPly 913	9
1.2.2 Results – Material: IS400	12
1.3 Discussion of experimental results	13
1.4 Conclusions	15
2 WP Multi-ply expansion	15
2.1 Methodology	15
2.2 Material characterization/ Material models	15
2.3 FE modelling / Model calibration/ Multi-ply approach	17
2.3.1 FE model	17
2.3.2 Simulated tensile and bending test	17
2.3.3 Dynamic-mechanical analysis	19
2.3.4 Three step modeling approach	20
2.4 Conclusions	22
3 WP Multi-axiality expansion	23
3.1 Experimental tests	23
3.2 Numerical modeling – fracture and damage analysis	25
3.2.1 FE model and material properties	25
3.2.2 Simulation results	26
3.3 Conclusions	30
References	31
Potential impact and main dissemination activities and exploitation results	31
Address of project public website and relevant contact details	32

Executive Summary

The FATIMA project consortium worked on testing and fatigue prediction of fiber reinforced plastics (FRP). The challenging objective was to go beyond the state of the art in terms of approaches to account for humidity, multi-ply, and multi-axiality effects in organic laminate structures.

Objective of FATIMA project was the adaptation and expansion of a methodology of accelerated fatigue testing and predicting of the lifetime of organic fiber reinforced structures, which has been introduced and comprehensively been described by Miyano.

Successful feasibility study of the existing methodology was carried out with the material IS 400, a typical epoxy based material with woven fiber reinforcement. The development of the methodology was achieved by applying dedicated tests, by using Digital Image Correlation (DIC) methods, and advanced simulation techniques in order to expand the existing methodology towards humidity influence, multi-ply and multi-axiality effects.

The material was supplied by the Clean Sky ED-ITD partners and the tests were carried out in WP1 with equipment capable of varying temperature, frequency, and load amplitude. Thereby the effect of temperature dependent static, transient, dynamic and fatigue contributions was analyzed. The methodology is performed based on three kinds of tests: viscoelastic dynamic mechanical analysis (DMA), constant strain rate (CSR), and cyclic fatigue tests at various temperatures, frequencies, and loading ratios. Modes of structural fatigue were analyzed and compared to the acceleration factors based on the viscoelastic time-temperature shift function. Thereby the new method was clearly revealing its great potential for predicting the critical number of cycles to failure and its dependency on temperature as well as the long term fatigue strength of fiber reinforces polymers including PCB materials.

The methodology enhancement with respect to multi-ply effects was developed and validated in WP2. After material characterization for the individual plies the visco-elastic properties of the epoxy matrix material were extracted and implemented in the FE simulation macros. Additionally, microscopic investigations delivered the necessary geometric parameters for simulation. After build-up of detailed 3-D finite element models tensile, bending and shear simulations were carried out. Calibration of 3-D numerical models were successfully accomplished and resulted in a good agreement of the effective Young's modulus with measured data. Additionally a good agreement of storage and the loss modulus was reached between simulation and experimental results obtained by dynamic mechanical analysis (DMA). In accordance with the multi-ply expansion approach a material characterization was simulated using a layered model. In the final step a full FRP stack was modelled according to the respective ply scheme.

After material characterization in WP1 and development of a toolbox for modeling FRP laminates in WP2 the methodology was expanded in WP3 to complex loading situations with combined tension and bending load. Therefore a specially designed specimen holder was used introducing a bending moment in addition to in-axis tension. Based on the experimental tests numerical simulations were performed to understand the multi-axial fatigue loads and the complexity of this combined load configuration. Finally, a number of failure criteria have been developed and tested for analyzing, describing, and predicting damage in composite materials due to multi-axial loads.

Summary description of project context and objectives

Objective of FATIMA project was the adaptation and expansion of a methodology of accelerated fatigue testing and predicting of the lifetime of organic fiber reinforced structures, which has been introduced and comprehensively been described by Miyano.

The development of the methodology was achieved by applying dedicated tests, by using Digital Image Correlation (DIC) methods, and advanced simulation techniques in order to expand the existing methodology towards humidity influence, multi-ply and multi-axiality effects.

Intensive work in the field resulted in a number of concepts for accelerated lifetime predictions for carbon fiber reinforced polymers. Within FATIMA, these concepts were adapted to the material provided by the partners of the Clean Sky consortium (IS400 and HexPly913). Thereby the field covered by the Miyano methodology was substantially extended towards fast and cost-efficient testing of airframe structures. Additionally expansions were approached addressing humidity effects, different stack-up structures, and combining loading (such as tension and bending or tension and torsion) on the lifetime of these composite materials.

First, the change in visco-elastic behavior of organic resins due to moisture adsorption had to be modeled by expanding the time/temperature shift function into a time/temperature/moisture shift function. Second, a tool box had to be developed for composing appropriate models of a specifically stacked laminate. Therefore all plies and structures within the stacked/woven laminate have to be considered and included in the final model. Finally, a number of failure criteria were developed for analyzing, describing, and predicting the damage in composite materials due to multi-axial loads. These had to be evaluated according to their applicability to the provided CFRP systems. Final goal was the definition of an appropriate failure criterion. Main challenge of the project was the adoption of these concepts and their integration into the methodology of fatigue testing.

The project was split into four work packages (WP): WP 1 - Humidity Expansion, WP 2 - Multi-ply expansion, WP 3 - Multi-axiality expansion, WP 4 - Project management and leadership. WP1 was dominated by experiments while the other two packages WP2 and WP3 were dominated by a combination of simulation and experimental work.

1. WP Humidity Expansion

Humidity Expansion addressed the determination of the effect of moisture content within the polymer matrix on the mechanical behavior and on the lifetime of FRP.

Main objectives:

- Characterization of sorption behavior of given sample material (humidity adsorption and desorption over time and temperature)
- Definition and specification of test conditions
- Evaluation of material in reference state, visco, strain rate, fatigue
- Quantitative determination of the effect of different humidity levels on visco-elastic behavior of the resin (effects on visco-elastic master curve and TTSE)
- Quantitative determination of the effect of different humidity levels on constant strain rate test results
- Quantitative determination of the effect of different humidity levels on fatigue test results
- Including the moisture effects into the fatigue model by introducing and quantifying another factor to the shift function resulting in the time-temperature-moisture shift function (TTMSF)

At all experimental stages, the tests were accompanied by state of the art characterization techniques concerning the physical failure analysis (x-sectioning, microscopy, 3-D X-ray tomography etc.). Scanning electron microscopy (SEM) imaging of failed specimen at crack area was carried out for detection of failure mechanisms (fiber matrix interface, matrix cracking, cohesion or adhesion dominated).

2. WP Multi-ply Expansion

Multi-ply Expansion addressed the establishment of a tool box for composing arbitrary laminate structures based on the ply types and orientations they consist of.

Main objectives:

- Physical analysis of plies contributing to the stack of the laminate structure and modeling representative sections of these plies in detail by parametric 3-D finite element meshes
- Experimental determination of the visco-elastic properties, strength, and fatigue behavior of individual plies and adjusting the material as well as the damage parameters by simulating the tests – DMA, constant strain rate, fatigue
- Transferring engineering parameters to effective models of plies and validating the model behavior by independent experimental tests
- Adoption of network and laminate theory to compose the model of full laminate structures based on the individual ply models and validation of simulation results concerning visco-elastic, strength, and fatigue behavior by tests of full stack samples

A tool box for composing arbitrary laminate structures based on the ply types they consist of was established. Starting point was a detailed characterization of the individual plies. Applying experimental and simulation techniques, visco-elastic properties, strength, and fatigue behavior of the single plies were determined. The extracted engineering parameters were then transferred to effective models of individual plies. Finally, the real structures were composed out of the effective ply models by combining network and laminate theories. All models were created based on closed loop combinations of experimental tests, physical analyses, and numerical simulations. In the first step, the engineering parameters were identified and determined for a number of cases defined by a design of experiment (DoE) plan covering the design space according to the options of the material provided by the Clean Sky partners. Afterwards, additional tests were performed to validate the findings at different positions within the design space independently.

3. WP Multi-axiality Expansion

Multi-axiality Expansion addressed the expanding of the existing methodology to complex load situations simultaneously combining several contributions like tensile, shear, and torsion.

The existing methodology of predicting fatigue in fiber reinforced laminates can be applied to any type of uniaxial load situation such as bending or tension. However, real situations are typically characterized by multi-axial loads, in which a mixture of bending, twisting, and tension or compression acts on the structure simultaneously. Hence, the existing methodology shall be expanded in order to avoid compromises like choosing one dominating load direction and neglecting all others. This expansion marks the objective of this WP 3. It was based on known failure criteria such as maximum strain / stress, Hashin and Puck. The applicability, validity, and accuracy of the criteria were assessed in order to identify the best fitting or to derive an even more suitable new criterion. Assessment work was carried out by combining numerical simulations with experimental test and characterization techniques. The simulations utilized FE analysis based on continuous and fracture mechanics approaches. They covered a representative sample while being loaded in several stress and fatigue tests. The computational results were compared to experimental readings of exactly those tests. This allowed calibrating the models the simulation is based on.

Main objectives:

- Specification of uniaxial and well defined multi-axial stress and fatigue tests for CFRP laminates with various strain rates at different temperatures
- Performing the stress tests and recording the evolution of the forces and the 2-D deformation fields vs. time; generating dynamic strain maps from the surfaces of the specimen (from unidirectional plate)
- Assessing the stress tests by numerical simulation based on models calibrated, verified, and validated by experimental readings

- Identifying an appropriate failure criterion to be implemented into the existing methodology of predicting fatigue of the CFRP laminates or deriving an even more suitable criterion
- Performing fatigue tests; determining the experimental lifetime; comparing to lifetime estimation based on simulation results applying the expanded methodology according to the task before

4. WP Project Management and Leadership

The main objectives of the WP Project Management and Leadership are:

- Provide leadership and project management to the task and partners
- Adjust activities in various WPs, interact with WP leaders
- Act as intermediate between project partners and European Commission
- Identify potentially exploitable technologies arising from research and manage IPR issues

Project Management organized work and co-operation between the partners within the various. All reports (technical, financial, management) and deliverables required by the European Commission were delivered in time. Furthermore dissemination and exploitation of results and IPR issues was organized and carried out.

Description of main S & T results/foregrounds

1 WP Humidity Expansion

1.1 Methodology

Since FRP materials show a strong time and temperature dependency, the approach of simply applying S–N curve to polymer composites as it would be done with metals, cannot provide accurate prediction of the FRP fatigue life. Accelerating the test of polymer composites is nevertheless possible with applying the testing methodology developed by Miyano et al. [2, 3]. This methodology is based on three kinds of tests: viscoelastic dynamic mechanical analysis (DMA), constant strain rate (CSR), and cyclic fatigue tests. It rests on the hypothesis that the viscoelastic behavior of the FRP materials is fully determined by the polymer resin and not affected qualitatively by the reinforcing fibers. Therefore, the time-temperature superposition (TTS) principle, which is determined by the usual viscoelastic DMA material characterization of polymer resins, also controls the response to the load and the time to failure, i.e., the fatigue behaviour, of complete and complex FRP materials.

Originally, the method has been introduced for unidirectional laminate structures. In this case, elevated temperature states were used to accelerate the mechanical degradations, which occur under loads over long period of time at lower temperature [2, 3].

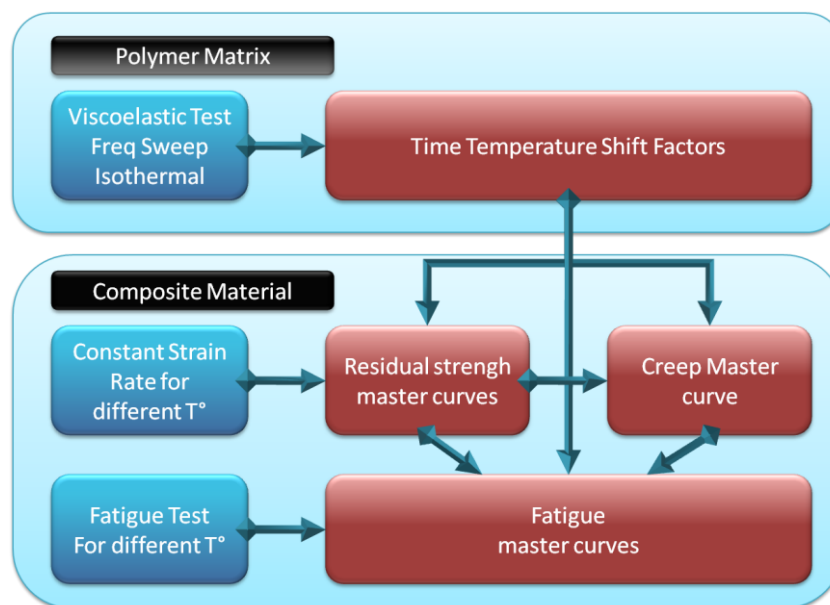


Figure 1: Outline of the accelerated testing methodology

Figure 1 shows the outline of the accelerated testing methodology. It also applies the premise that the failure mechanisms under CSR, creep, and cyclic fatigue loadings are identical. Consequently, all three loading types may be interlinked to contribute to the fatigue behavior:

- The creep loading can be considered as a fatigue loading with stress ratio of $R = \sigma_{\min}/\sigma_{\max} = 1$.
- The CSR loading can be taken as equivalent to a half cycle of fatigue loading with $R = 0$.

In the well known DMA approach, a shift factor of 1 is assigned to a suitably chosen reference temperature while the test results at all other temperatures are shifted along the logarithmic scale of time until they form a smooth curve. The amounts of these shifts determine time/temperature shift factors, which are condensed into a time/temperature shift function (TTSF).

According to the fundamental hypothesis, the same time-temperature superposition principle holds for all three types of strengths (CSR, creep, and fatigue). This means that it is possible to use the same TTSF for all three types of strengths. Hence, master curves are not limited to the viscoelastic behavior but also valid for the static CSR strength and the cyclic fatigue strength, respectively – always applying the same TTS factors as found in the viscoelastic DMA master curve.

In addition, a second hypothesis states that the linear cumulative damage law can be used for monotonic loading. This allows estimating the life under complex loading, by summing up the damages for individual load steps and to build up the creep strength master curve. Finally, a third hypothesis states the linear dependence of fatigue strength upon the stress ratio R : Using this hypothesis, fatigue master curves for various stress ratio values can be generated.

1.2 Experimental Procedure

In this project the validity of the procedure introduced by Miyano et al. [3] was established for the two sets of FRP materials (HexPly913 and IS400). The expansion of the methodology for predicting the lifetime under various loading conditions had to be demonstrated at these materials.

Therefore samples were cut out of a larger piece of FRP films with the dimension of 50 x 3 mm². Specimen thickness was 0.68 mm for HexPly 913 and 0.96 mm for IS400, respectively. Thermo-mechanical properties of both materials were then measured using a DMA (Explexor 100N from Gabo), a static tester (Zwick 1446), and a dynamic tester (QTron 250 from MTS). Master curves were constructed by shifting the curves on the logarithmic frequency scale by the shift factor A [3]. The respective values for the shift function could be fitted with the Arrhenius function (eq. 1):

$$\log A = -\frac{\Delta H}{2.303 R} \cdot \left(\frac{1}{T} - \frac{1}{T_{REF}} \right) \quad (1)$$

where R is the gas constant of $8.314 \cdot 10^3$ kJ/(K mol), H is the activation energy, T_{REF} is the reference temperature, for which room temperature was chosen, and T is the actual temperature the results were obtained at. The viscoelastic characterization was completed when obtained parameters could be used as, for example in eq. 2, for the storage part of the Young's modulus E' :

$$E'(t) = E'_\infty + \sum_{i=1}^N E'_i \exp\left(-\frac{t}{A(T, T_{REF}) \tau(T)}\right) \quad (2)$$

where E'_∞ is the modulus at rubbery state, E'_i and τ_i denote the i^{th} of N sets of Prony parameters (modulus and time constant, respectively), and t is the time.

1.2.1 Results – Material: HexPly 913

DMA: Samples were measured in a DMA under various frequencies (0.5; 1; 5; 10; 50 Hz) with temperature steps of 5°C between -40°C and 260°C (frequency sweep at isothermal temperature). The resulting curves of storage modulus and phase angle ($\tan \delta$) are shown in Figure 2.

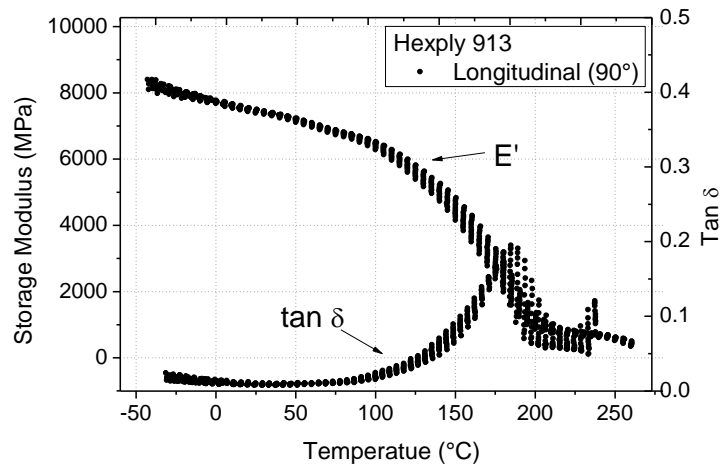


Figure 2: Viscoelastic properties of HexPly 913

The master curve was obtained from the DMA curves by assuming thermo-rheological simplicity and invoking the principle of TTS. The viscoelastic master curve and the TTSF for HexPly 913 are represented in Figure 3 and Figure 5, respectively.

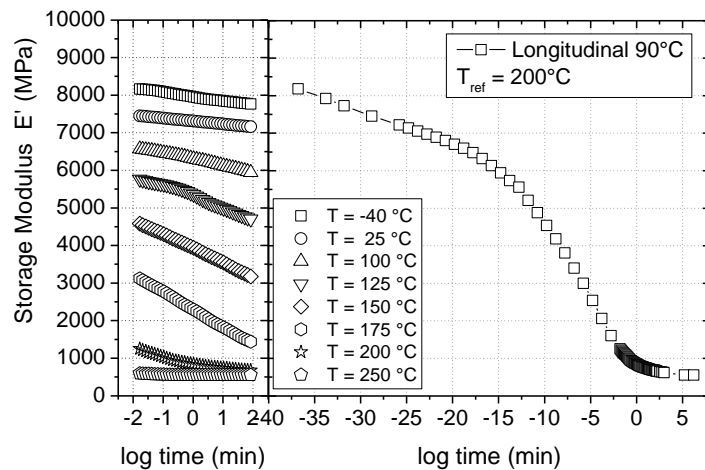


Figure 3: Viscoelastic master curve of HexPly 913

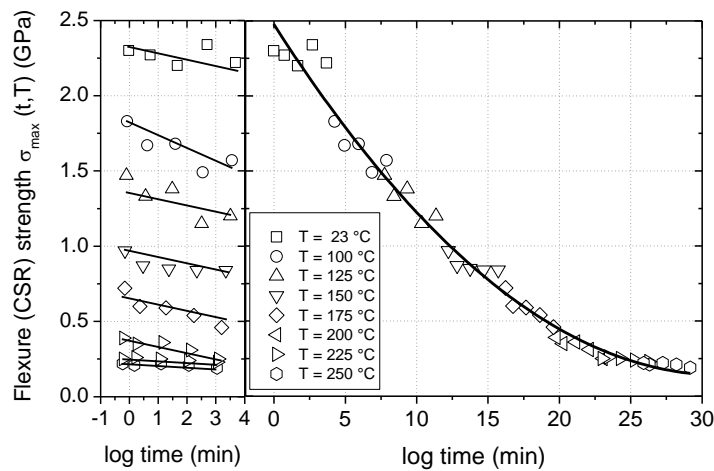


Figure 4: CSR Master curve obtained from CSR curves (left), HexPly 913 (Ref. temperature = 23°C)

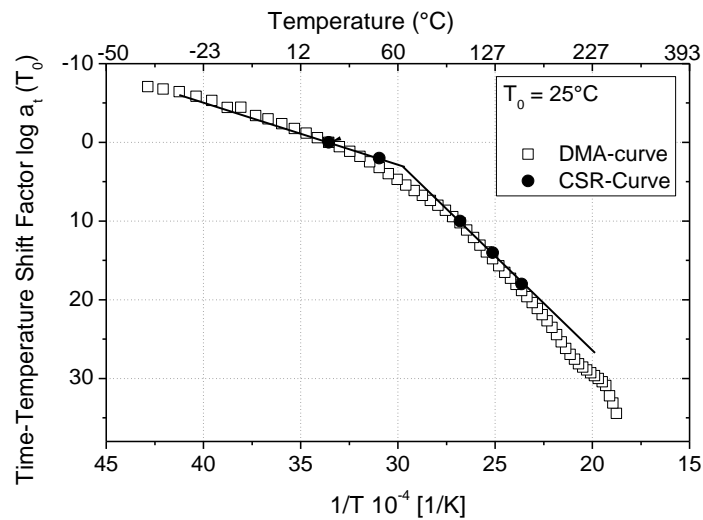


Figure 5: Time-temperature shift function obtained from viscoelastic (DMA) and from CSR curves, HexPly 913

CSR: The constant strain rate curves were obtained using the Zwick machine with 10 kN load cell in 3 point bending configuration. Measurements were done using (0.001; 0.01; 0.1; 1.0; 10 mm/min) as speed of the measurement head at temperature steps of 25°C between room temperature up to 250°C. The CSR curves and the master curve obtained by applying the viscoelastic TTSF are shown in Figure 4. In addition, Figure 5 also indicates the perfect match between the viscoelastic TTSF and that generated by shifting the CSR results of the various temperatures until a smooth master curve is formed. The coincidence of the two independent TTSF supports the validity of the fundamental hypothesis of the accelerated testing methodology.

Fatigue test: Fatigue bending tests were performed at two different temperatures (room temperature, 100°C), a load ratio R of 0.05, and a cycle frequency of 2 Hz using an MTS equipment in 3 point bending configuration. The results are shown in Figure 6

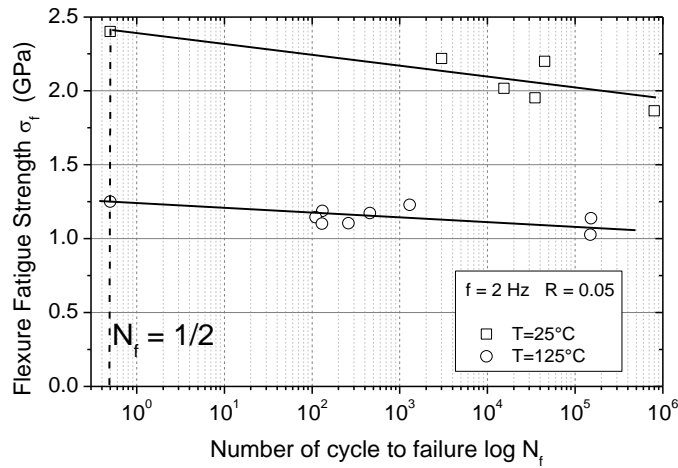


Figure 6: Number of fatigue cycles to failure for HexPly 913

1.2.2 Results – Material: IS400

The procedure of assessing the material HexPly 913 was also applied for testing the epoxy based material IS400, which is commonly used in printed circuit boards (PCB).

DMA: The dynamic mechanical analysis was carried out in form of frequency sweeps between 0.5 Hz and 50 Hz at isothermal temperatures in steps of 5°C between -40°C and $+250^\circ\text{C}$ in order to obtain viscoelastic data (Young's modulus and phase angle, $\tan \delta$) and - most of all - the TTSF of the PCB material IS400. The result is plotted in Figure 7

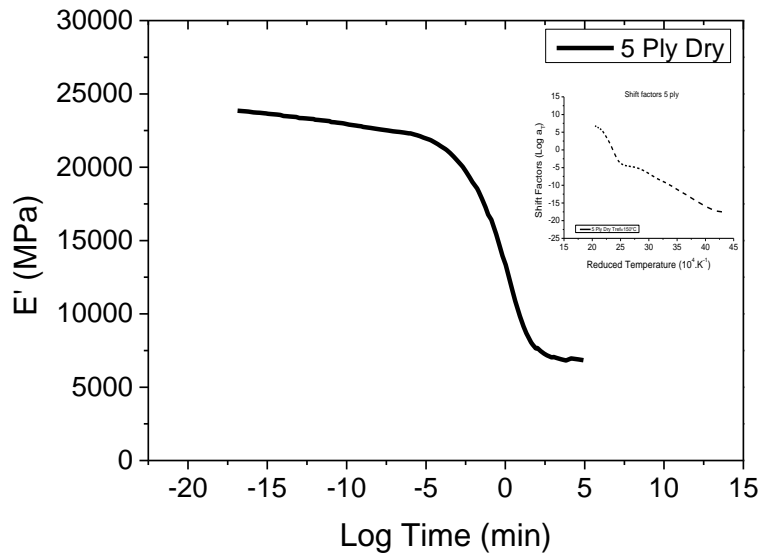


Figure 7: Viscoelastic Master curve and corresponding shift factors of the material IS400

CSR: The constant strain rate results were obtained by determining the ultimate strength of the IS400 samples in 3 point bending configuration for seven different temperatures between room temperature and 200°C and at four different speeds of the measurement head (0.001; 0.01; 0.1; 1.0 mm/min). The results of the measurements and the resulting master curve are shown in Figure 8.

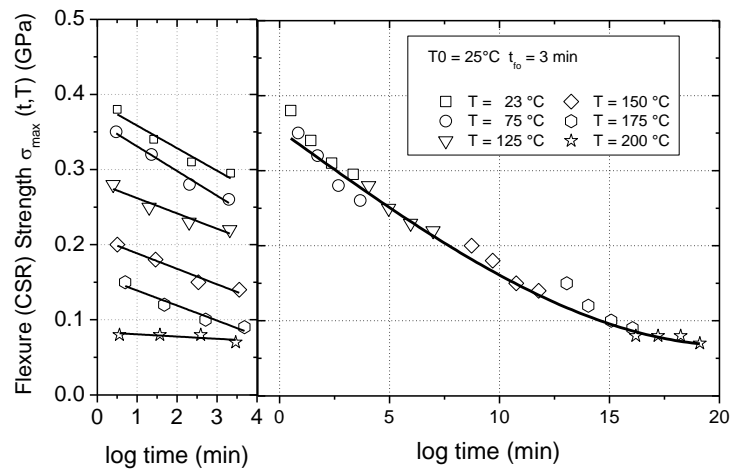


Figure 8: CSR curves and CSR master curve, IS400

Fatigue test: The cyclic bending fatigue of IS400 was assessed at a frequency of 2 Hz and a load ratio R of 0.05. In case of the PCB material, five different temperatures between room temperature and 150°C were considered by the test. This exceeds the number chosen for the reference material HexPly 913 because the focus of this study has been to show the validity of the accelerated testing methodology for PCB materials. The numbers of cycles to failure obtained by these tests are represented on Figure 9.

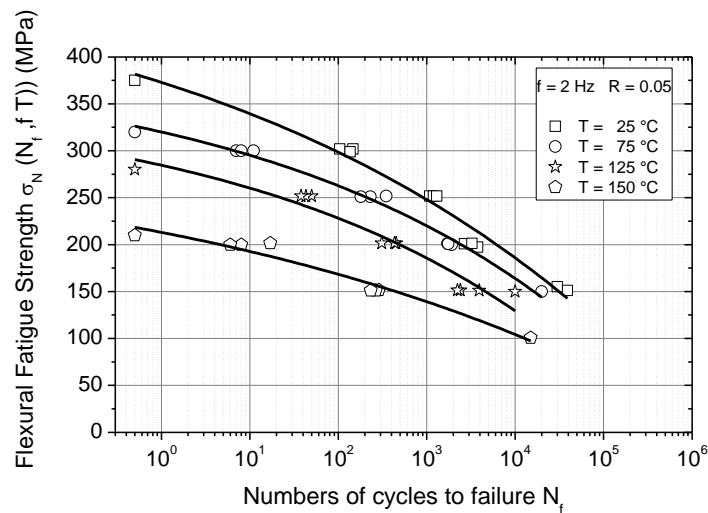


Figure 9: Number of cycles to failure for various temperatures, IS400

The material IS400 shows a lower magnitude in fatigue strength than the reference material HexPly 913. In addition, the dependence of the number of cycles to failure on the force applied is stronger. Hence, the measurement of IS400 leads to more reproducible results showing less scatter.

1.3 Discussion of experimental results

Physical failure analysis of the samples after CSR and cyclic fatigue tests revealed delamination at the interface between fibers and resin with the subsequent fracture of the fibers as cause of failure in all instances. Therefore, the premise of identical failure mode is fulfilled by both materials, HexPly 913

and IS400. Hence, it is well possible to construct a fatigue master curve. It started with applying the valid premise, i.e., by interpreting the CSR master curve as the limiting case of the failure already occurring during the very first load cycle. Then, the results of the cyclic fatigue tests were added. They formed branches starting at the CSR master curve and progressing towards higher number of cycles to failure and lower forces. The shifting of the individual fatigue curves was done according to the TTSF, which was obtained by the viscoelastic DMA and confirmed by the analysis of the CSR tests. Finally, the levels of the individual fatigue curves denoting 10; 100, 1000, and 10000 cycles to failure, respectively, were linked by thin solid lines.

Figure 10 shows the fatigue master curve for the PCB material IS400 based on the fatigue tests at room temperature, 125 °C, and 150 °C. This fatigue master curve may now serve as graph for estimating the structural fatigue lifetime of the PCB material at any temperature and under various types of loads (static / constant strain rates ... dynamic cycles).

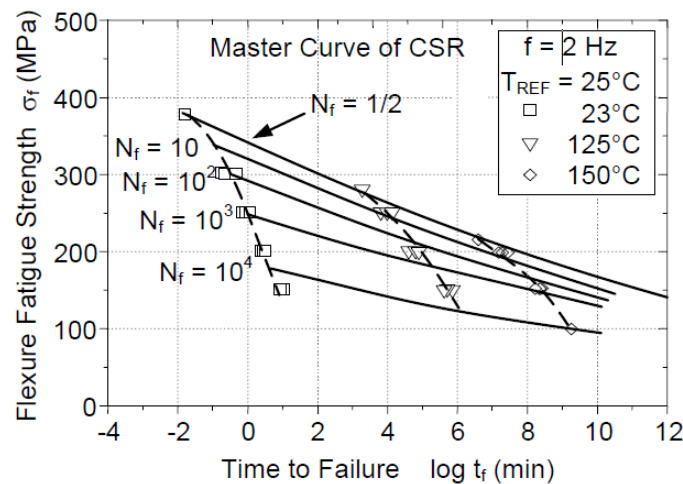


Figure 10: Fatigue master curve for PCB IS400

The analysis shows that the methodology developed by Miyano et al. [3] is well applicable to both materials assessed, i.e., to the reference avionic material HexPly 913 and to the PCB material IS400. As demonstrated above, this methodology is capable of providing the means for performing accelerated lifetime tests, which even result in a fatigue master curve that allows to estimate the structural lifetime across quite a field of load cases not all been tested directly: The measured viscoelastic properties of the two materials using DMA in frequency sweep at isothermal steps for a large panel of frequencies led to the viscoelastic master curves and provided the TTSF for the results of CSR and cyclic fatigue tests as well since the failure mechanisms were the same for all three tests. Therefore, it was possible to create smooth master curves of the static strength and cyclic fatigue based on static tests with constant strain rates and dynamic tests with constant frequency, both at various temperatures, respectively. To finish, a master curve of creep strength could also be created by using the second and the third hypothesis as listed before.

The developed methodology is seen as valuable tool for keeping the testing efforts in reasonable effort even in cases of FRP being exposed to severe structural loads. Hence, this methodology will most likely become very relevant for the development of future applications.

In this chapter, we have presented and discussed the results of viscoelastic, constant strain rate, and fatigue tests at various temperatures, frequencies, and loading ratios. The modes of structural fatigue were analyzed and compared to the acceleration factors based on the viscoelastic time-temperature shift function. This way, the new method was clearly revealing its great potential for predicting the critical number of cycles to failure and its dependency on temperature as well as the long term fatigue strength of fiber reinforced polymers including PCB materials.

1.4 Conclusions

The WP1 addresses the determination of the effect of humidity on the long-term fatigue strength of IS400 FRP laminates. IS400 laminates were conditioned in humid atmosphere at 85% RH / 85°C for at least 96 h prior to visco-elastic and fatigue tests.

According to sorption-desorption measurements, full saturation was reached this way. In an early phase of the project, 3-point bending DMA tests in frequency sweep / temperature step mode were carried out on dry samples in order to build the reference master curve and shift factors of the visco-elastic behavior. For the saturated IS400 samples, a different procedure had to be applied in order to prevent the samples from drying during measurement. By means of fast tests with a continuous temperature ramp at one frequency per sample, it was as well possible to determine the visco-elastic master curves and shift factors of these moisturized FRP samples even with T_g as high as 135°C. Afterwards, a series of constant strain rate measurements for various temperatures have been executed. These measurements were then used to build a master curve.

2 WP Multi-ply expansion

2.1 Methodology

The characterization of FRPs requires time-consuming and hence expensive tests due to their visco-elastic behaviour. On the basis of such experiments, so-called master curves can be created that provide the information about the time-temperature behaviour comprehensively. Beyond the visco-elasticity, immense time-consuming experiments are necessary to describe the fatigue and failure behaviours of such materials. To avoid this huge variety of experiments, the method developed by Miyano et al [3] can be applied. It is based on the principle that the ultimate strength and the fatigue behaviour of FRP materials also follow the time-temperature shift as determined by the visco-elastic analysis. The Miyano method allows the creation of strength and fatigue master curves based on a limited number of experiments. By means of them, it is possible to determine mechanical characteristics such as storage modulus, strength, and fatigue under different combinations of loading frequency, temperature and stress ratios. However, all these master curves are only valid for the respective investigated FRP materials with exactly their number and types of plies. They need to be repeated as soon as a ply is added or removed to or from the investigated material. In order to avoid this repetition of tests, a toolbox based on the finite element method was created that can reduce the time-consuming and cost-intensive effort during determination of behaviour of failure as it allows covering FRPs with different stack configurations based on a fraction of tests originally needed. The toolbox realizes an accelerated characterization of the FRP's behaviour of failure for lifetime assessment of arbitrary laminate stackings based previously characterized individual layers.

2.2 Material characterization/ Material models

The FRP material IS 400, a typical fiber-plastic composite, has been characterized. Figure 11 and 12 show the corresponding flexural visco-elastic master curves and shift functions of the characterized single plies, 5- and 10 identical plies. The absolute stiffness rises with the number of plies as seen in Figure 11 by means of the visco-elastic master curves obtained from bending tests of 'dry' samples. However, the TTS (time temperature shift) of all three samples is almost identical. The gray shadow curve in Figure 12 indicates the average of the three TTS curves. Obviously, the time dependency of the elastic response to mechanical loads is qualitatively independent of the number of plies. Moreover, the multi-ply TTS function also holds for the onset of failure in CSR tests. The symbols added to Figure 12 mark the shift factors determined by the CSR tests of samples with 5 and 10 plies, respectively. They coincide very nicely with the visco-elastic multi-ply TTS curve plotted as solid lines. This demonstrates the applicability of the proposed accelerated lifetime test.

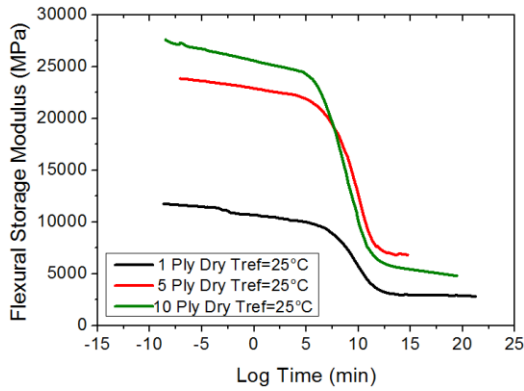


Figure 11: Flexural visco-elastic master curves of IS-400 – 1, 5, and 10 plies

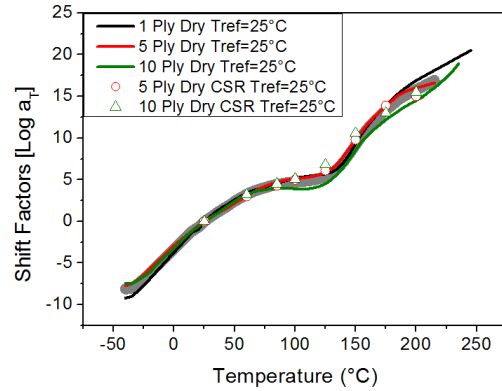


Figure 12: Shift functions for the flexural visco-elastic and CSR master curves of IS-400 – 1, 5, and 10 plies

Cross sections of a 5-ply laminate were carried out to get real geometry values. Figure 13 and 14 represent the cross section parallel to the x-z plane and across the fibers, respectively. Microscopy images serves as the basis for the dimensions of the fiber bundles, the distance of the fiber bundles and the fiber diameter. These dimensions were used for the finite element geometry modeling.

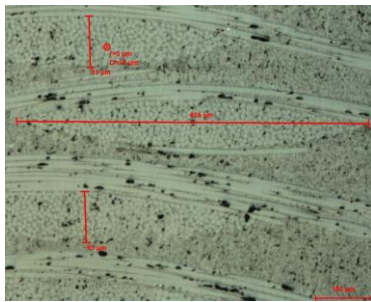


Figure 13: Cross section of FRP IS 400 parallel to X-Z plane

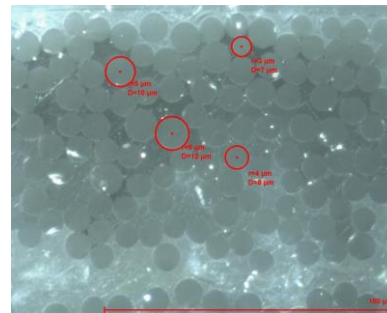


Figure 14: Cross section of FRP IS 400 across the fibers

The elastic and visco-elastic properties of the matrix material determined experimentally were applied to the FE simulations. The material data of the glass fibers are well-known and were taken from literature [4].

The fibers are introduced in the FE model as an elastic material and the matrix as a visco-elastic material in terms of PRONY series (3, 4).

$$G = G_{\infty} + \sum_{i=1}^{n_G} G_i \exp\left(-\frac{t}{\tau_i^G}\right) \quad (3)$$

$$K = K_{\infty} + \sum_{i=1}^{n_K} K_i \exp\left(-\frac{t}{\tau_i^K}\right) \quad (4)$$

$$\log a_T(T) = \frac{C_1(T - T_0)}{C_2 + T - T_0} \quad (5) \quad a_T(T) = A_n T_n + A_{n-1} T_{n-1} + \dots + A_2 T_2 + A_1 T + A_0 \quad (6)$$

Due to the time-temperature shift of the relaxation functions at different temperatures the master curve is generated (see WP1). How much each separate relaxation function have to be shifted is determined by the so-called shift function $a_T(T)$. An analytical approximation of this function is given by the Williams-Landel-Ferry (WLF)-equation (5) or polynomial function (6).

2.3 FE modelling / Model calibration/ Multi-ply approach

2.3.1 FE model

The aim of the toolbox comprehends the adaption of the viscoelasticity that is the time dependent behavior of the polymer [5]. Polymer and reinforcing fibers are addressed separately. Regular hexahedral volume elements (SOLID185 [6]) are used for the visco-elastic polymer matrix, which is isotropic. The time independent glass fibers are modelled either by a second set of hexahedral elements or by special reinforcement elements (REINT265 [6]). In both cases, the two sets of elements are tightly coupled by using identical nodes. Having the stiffness assigned in fiber direction only, the second set of elements turns the visco-elastic reaction of the complete FRP ply into a highly anisotropic one as it is in reality. Figure 5 depicts the detailed 3-D model that is used for simulation of tensile (A), shear (B) and bending (C) load.

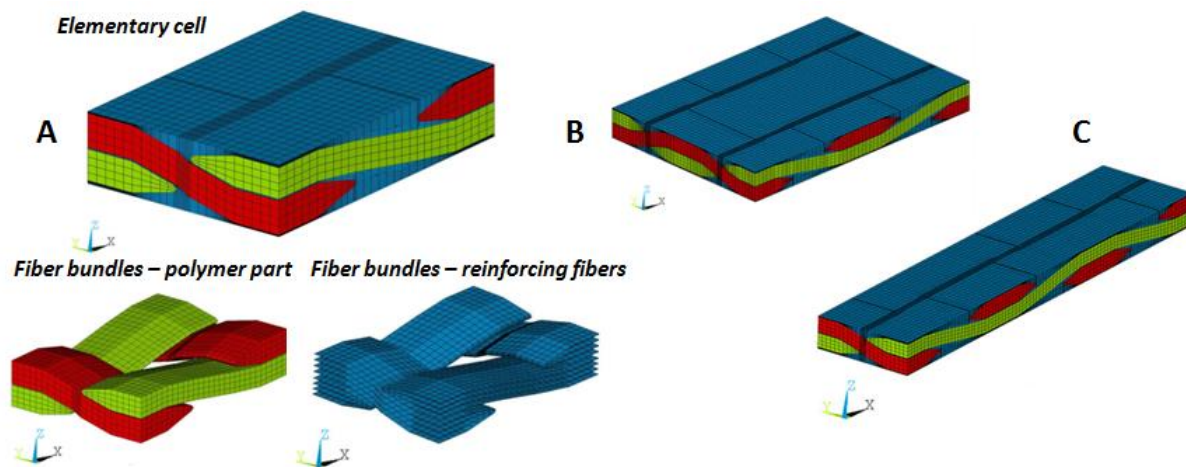


Figure15: Modeled basic cell for simulation of tensile (A) shear (B) and bending (B) test

The hexahedral elements represent the polymer outside (blue), and within the fiber bundles (red and green), respectively. The shell-like elements also seen in Figure 15 represent the glass fibers. The stiffness of the polymer elements is adjusted according to the resin content, which is considerably lower than 100% inside the fiber bundles and may even be specific to each fiber direction. All dimensions are input as parameters so that the model can easily cover any known ply type. The detail model is now able to replicate the local 3-D deformation and stress fields within the elementary cell of a smart lightweight structure very precisely. One cell (Figure 15 A) already suffices for performing virtual tension tests, by means of which the parameters of the fiber dimensions are calibrated.

2.3.2 Simulated tensile and bending test

The first step of the calibration is performed using the 3-D detailed model. Under the applied tensile strain of 0.05% a reaction force F_R is computed at the master node and the effective Young's modulus can be calculated (7). The calibration of the fiber volume fraction is realized by approximation of the calculated effective E-modulus to the measured reference value. For this purpose, the ANSYS command SECDATA is used. The parameter fiber cross-sectional area and fiber spacing are input by this command and internally converted into height of the reinforced layer h_{reinf} (8). Therefore it is useful to define one of the two values as a constant and the other to use for calibration.

$$E_{eff} = \frac{F}{A \cdot \epsilon} \quad (7)$$

$$h_{reinf} = \frac{A_{Fiber}}{S_{Fiber}} \quad (8)$$

The cross-sectional area A_{Fiber} is defined to be constant, therefore the value to calibrate is the fiber spacing S_{Fiber} . In the result of the calibration steps an appropriate value in x and y direction was found. Figure 16 shows the additionally used geometry parameters to fit the calculated E_{eff} .

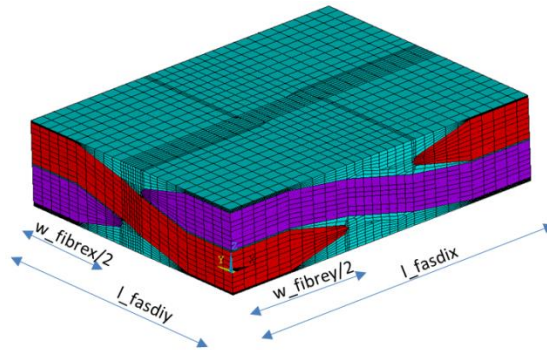


Figure 16: Geometric fit parameters at the 3-D detailed model

The stress analysis is important for the evaluation of finite element model used. The stress distributions are consistent and the location of the stress maxima and minima are in agreement with the expected locations (see Figure 17-18).

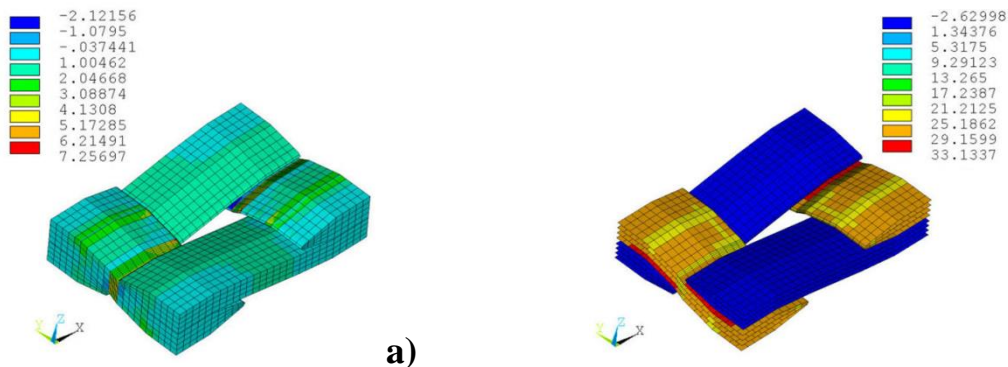


Figure 17: σ_{yy} as a result of y-tensile load; a) in the epoxy resin of the glass fiber bundle; b) in the REINF-elements modeled the glass fibers

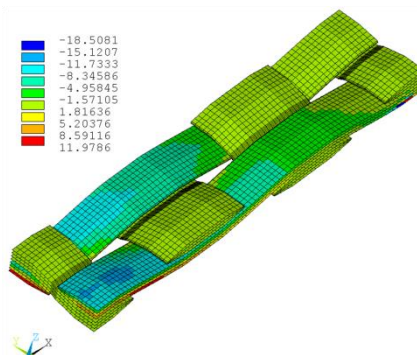


Figure 18: σ_{xx} as a result of bending load along the x-axis in the REINF-elements modeled the glass fibers (complete symmetric 3-point bending model)

As described above, the effective fiber spacing S_{eff} could be calibrated for the glass fiber bundles in the x and y direction so that the effective E-modulus is approximately equal to the measured values in both directions. To validate these results, a 3-point bending test is simulated along the x and y axis. Table 1 und 2 demonstrate a good agreement between effective E-moduli extracted from measurement and simulation and the comparison mostly resulted in a difference less than 5%. A reason of the moderately higher difference concerning the 3-point bending test could be the application of the 8-node solid element type that is less suitable for bending applications in comparison to higher order elements that exhibits quadratic displacement behavior. Here, an agreement had to be found because of the significant higher calculation time under using 20-node elements.

	Eff. fiber distance	Distance of the X fiber bundles' middle	Distance of the Y fiber bundles' middle	Width - X fiber bundles	Width - Y fiber bundles	E-modulus	E-modulus
	d_eff_x=d_eff_y	l_fasdix	l_fasdiy	w_fibrex	w_fibrey	E _{eff}	E _{eff}
	[mm]	[mm]	[mm]	[mm]	[mm]	[MPa]	[MPa]
Measured	/	0.853	0.565	0.579	0.593	20070	16140
Set	1.380E-03	0.8	0.62	0.56	0.625	19769	15788
Deviation [%]		-6.2	9.7	-3.3	5.4	-1.5	-2.2

Table 1: Comparison of measured and calculated E_{eff} by tensile test

	Eff. fiber distance	E-modulus	E-modulus
	d_eff_x=d_eff_y	E _{eff}	E _{eff}
	[mm]	[MPa]	[MPa]
Measured	/	6650	6300
Set 1	1.10E-03	6172	6013
Deviation [%]		-7.2	-4.6

Table 2: Comparison of measured and calculated E_{eff} by bending test

2.3.3 Dynamic-mechanical analysis

For analysis of the behavior of a viscoelastic material, both the temperature dependence and the time dependence have to be considered. These investigations can be done by relaxation tests or Dynamic mechanical analysis (DMA) at different temperatures. However, since the DMA delivers more characteristics such as storage and loss modulus this type of analysis is preferable to the relaxation tests if it comes to fatigue strength analysis. Moreover, the detailed model also captures the viscoelastic behavior in the DMA tests very well. Figure 19 and 20 compare the results of the virtual three-point bending test performed by numerical simulation applying the detailed model as seen in Figure 15 to the experimental data. The shift towards higher temperatures with the increase in loading frequency is likewise seen in both sets of results.

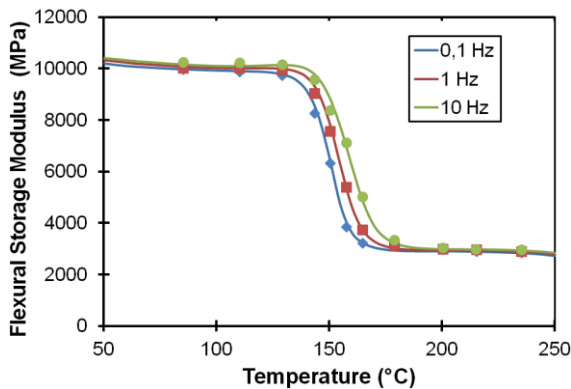


Figure 19: Virtual (simulated) DMA bending test of single ply specimen – storage modulus

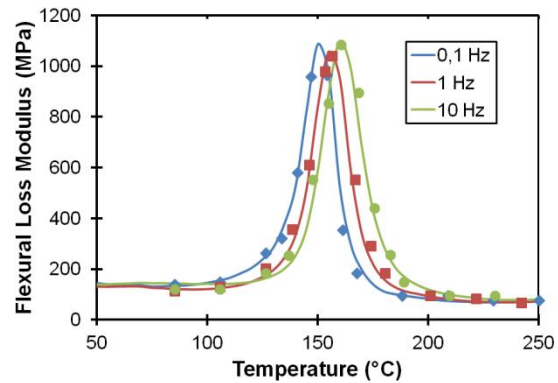


Figure 20: Virtual (simulated) DMA bending test of single ply specimen – loss modulus

Thereby the oscillating reaction force at the master node is used to calculate the effective storage modulus E' by equation (4) at $\sin(\omega t) = 1$ as well as the loss modulus E'' at $\cos(\omega t) = 1$. The maximum of the loss modulus and the maximum of the decrease of the storage modulus are gained in the region of the glass transition temperature. This maximum occurs at different temperatures dependent on the frequency.

Stress and strain are plotted over time in Figure 21 in which a phase shift (loss factor) occurs between both curves. In the case of the considered FRP the influence of the elastic fibers are dominating so that even in the range of the glass transition only a small loss angle exists. Consequently, the viscous part of the model is low under tensile load in this simulation. Figure 22 shows the stress-strain curve using the example of tensile load in x-and y-direction. In this case the model is loaded by a frequency of 0.1 Hz at a temperature of 107 °C, the temperature of the maximum loss modulus.

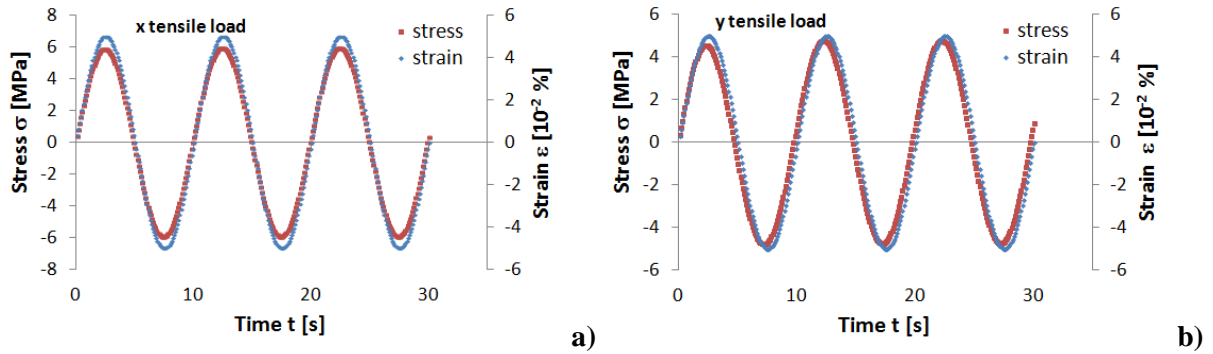


Figure 21: $\sigma = f(t)$ under tensile load at load frequency of 0.1 Hz at 107 °C;
 a) Tension in x direction; b) Tension in y direction

If the stresses and strains shown in Figure 22 are plotted against each other the hysteresis curves form. The shape of the curves depends on the loss angle δ . Due to the stronger viscous behavior in the y-direction and the associated larger loss factor two strongly different characteristics arise.

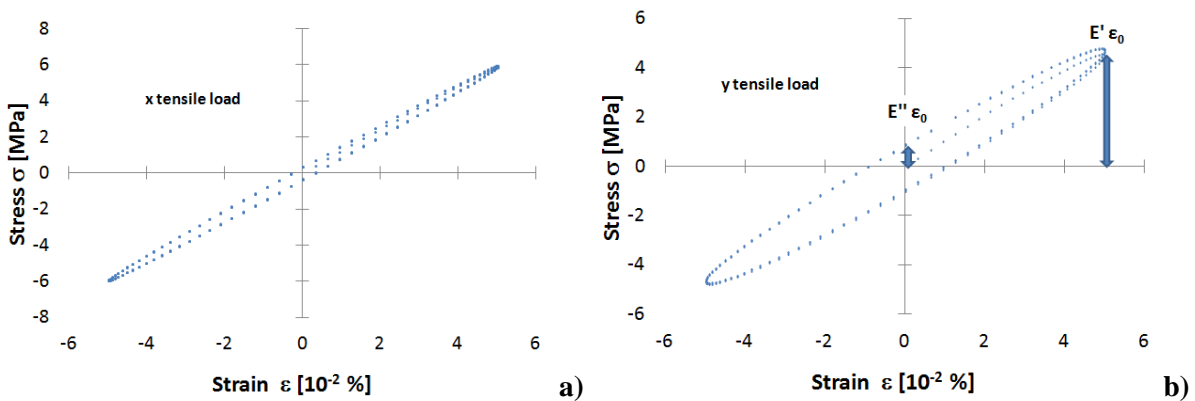


Figure 22: $\sigma = f(\epsilon)$ under tensile load at load frequency of 0.1 Hz at 107 °C;
 a) Tension in x direction; b) Tension in y direction

2.3.4 Three step modeling approach

The quantitative dependency of the stiffness from the number of plies can be covered by a numerical model. It follows the 3-steps concept depicts in Figure 23.

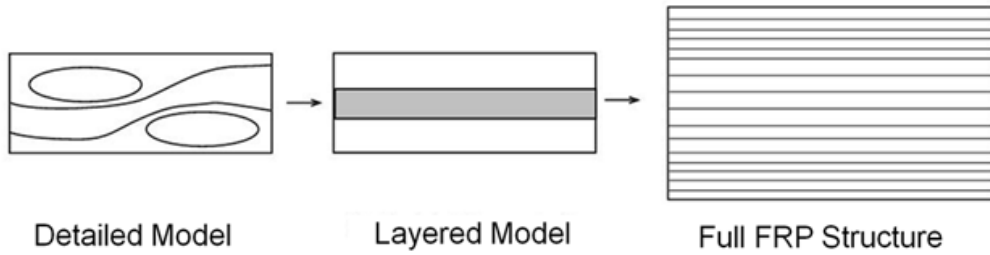


Figure 23: Three step modeling approach

First, the behavior of the single ply is studied at a representative FRP cell by means of a 3-D detailed model as described above. Afterwards, the laminate theory is applied to transfer the material data obtained in the first step to a simplified layered model. In the third step, the respective layer models are stacked according to the ply scheme so that the stiffness of the full FRP structure can be computed (Figure 23).

Thus, the detailed model can be used for determining the engineering stiffness values of orthotropic specimen (Young's modulus: E_{11} , E_{22} , E_{33} , Poisson's ratio: ν_{12} , ν_{13} , ν_{23} , and shear modulus: G_{12} , G_{13} , G_{23}). For this purpose the strains in x, y and z-direction are determined by tensile simulations in the three spatial directions. Whereas the effective Young's moduli can be determined by means of the reaction force at the master node according to equation (7) the Poisson's ratios results from negative ratio of transverse strain to longitudinal strain (9):

$$\nu_{xy} = -\frac{\epsilon_y}{\epsilon_x} \quad (9)$$

Determination of the other Poisson's ratios is performed respectively. From the shear simulations, the reaction force is determined at the master node and is used to calculate the shear moduli G_{xy} (10), G_{xz} and G_{yz} :

$$G_{xy} = \frac{F_x}{A_{xy} \cdot u_x} \cdot h_z \quad (10)$$

Because of the close match to the measured DMA data shown in Figure 19 and 20, the detailed model can act as benchmark when setting up a simplified layered model for each ply type. Eventually these models are stacked to form the complete lightweight structure, without losing the capability of accounting for visco-elastic effects. Applying the multi-layer feature of both element sets, the single FRP ply is modeled as a symmetric stack of polymer and reinforcing films. After calibrating, the simplified layer model (Figure 24) has the visco-elastic engineering stiffness values as listed in Tab. 3. They are in good agreement to the values of the detailed model validated by measurements.

$E_{11}' = 15.1 \text{ GPa}$	$E_{22}' = 15.5 \text{ GPa}$	$E_{33}' = 7.15 \text{ GPa}$
$E_{11}'' = 164 \text{ MPa}$	$E_{22}'' = 169 \text{ MPa}$	$E_{33}'' = 69.6 \text{ MPa}$
$G_{12}' = 1.34 \text{ GPa}$	$G_{13}' = 1.43 \text{ GPa}$	$G_{23}' = 1.42 \text{ GPa}$
$G_{12}'' = 12.9 \text{ MPa}$	$G_{13}'' = 13.5 \text{ MPa}$	$G_{23}'' = 13.3 \text{ MPa}$
$\nu_{12} = 0.103$	$\nu_{13} = 0.327$	$\nu_{23} = 0.326$

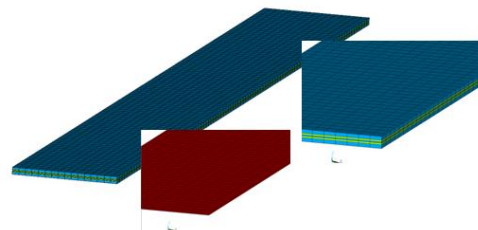


Table 3: Visco-elastic engineering stiffness values of a single IS 400-ply at room temperature **Figure 24 :** Layered model

Piling up the layered model according to the ply scheme, the full FRP stack is modeled in the final step (Figure 26). Additional features like interconnect lines, metal vias, and embedded components may now be introduced in addition (Figure 25).

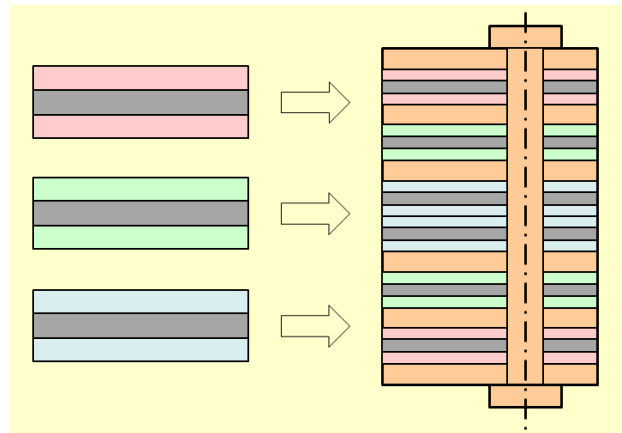
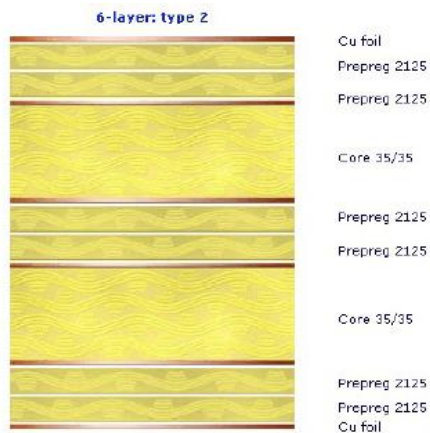


Figure 25 : Full stack example of a real structure (Source: electronic print Ltd. Co. KG) **Figure 26:** Third step of the three-step-modeling-approach- full stack

They complete the FRP model according to the real structure. They can also be used to compensate for some minor effects otherwise neglected by the simplified layer model, e.g., the small contribution the weaving of the fiber bundles may have onto the stiffness along the thickness of the laminate, i.e., normal to the ply area. Of course, the new quality now being covered by the model is fully kept. The FRP structure will realistically show the actual time dependency in the response to mechanical loads due to the behavior of the polymer matrix. This is true for the small scale responses like visco-elastic reactions but also holds for the large scale impacts ultimately leading to fracture and fatigue. Hence, the new modeling approach introduced in this work allows replicating the CSR and the fatigue master curves for a number of different stack configurations based on the data measured at the plies they consist of.

2.4 Conclusions

WP2 has addressed a tool box for composing arbitrary laminate structures based on the ply types they consist of. The IS 400 laminates were characterized in terms of different ply types and deliver the required material properties.

A three-step-modeling approach was developed and validated. In the first step it constitutes the basis of next steps a representative section of a ply was created in detail by parametric 3-D finite element models. It could be shown that the way of calibrating the detailed model by tensile tests and validating by bending tests is an effective and essential step in the development process. This process has to involve the transfer of the engineering parameters to the effective model of the ply followed by the calibration of the dynamic-mechanical behavior of the experimental tests and the appropriate simulations. Once these calibration steps were successfully performed, the laminate theory is applied to transfer the material data obtained in the first step to a simplified layered model as the second step. In the third step, the respective layered models were stacked according to the ply scheme so that the stiffness of the full FRP structure can be computed. The stepwise calibration enables the transfer of the mechanical behavior from the detailed model over a simplified layered model to a full stacked structure.

3 WP Multi-axiality expansion

3.1 Experimental tests

Following the concept proposed in the work package description, a specific specimen holder was designed according to [7] (Figure 27 a, b) and fabricated (Figure 27c). Design and realization had been executed in the time frame of WP3. Figure 27 d depicts the specimen holder in the mounted state.

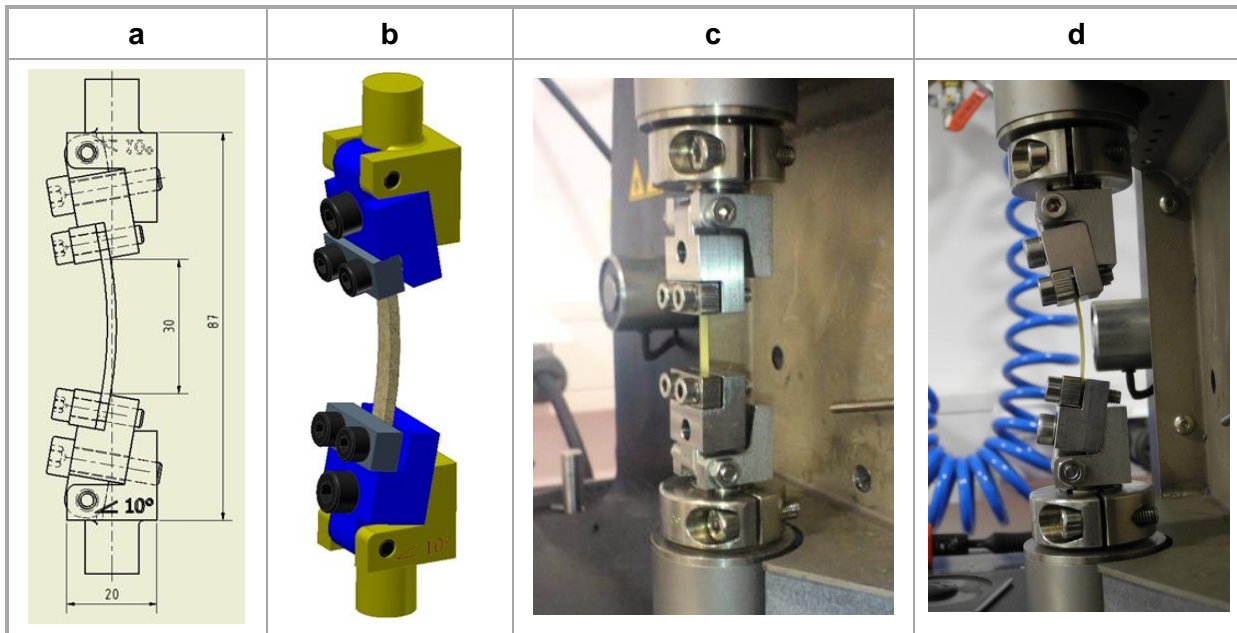


Figure 27: Engineering detail drawing (a, b) and mounted specimen holder (c, d) for combined tension-bending loading

The specimen is clamped into the grip, which is placed in a DMA machine (Figure 27 c). Then, the bending is applied by rotation of the clamping part (Figure 27 d) around 10° followed by a tensile step as shown in Figure 28.

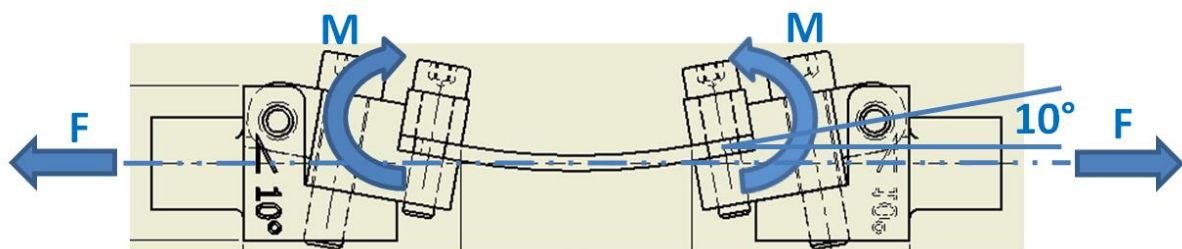


Figure 28: Loading by bending moment (1st step) and tensile force (2nd step)

Figure 30 shows force-displacement curves up to failure of the specimen. The fracture occurred directly at one of the edges at the fixed supports as depicted in Figure 29.



Figure 29: Fracture closed to the fixed support

This result is very similar to the published in [7]. The differences are caused on one hand by the shape of the specimen and on the other hand by the tensile force applied eccentrically.

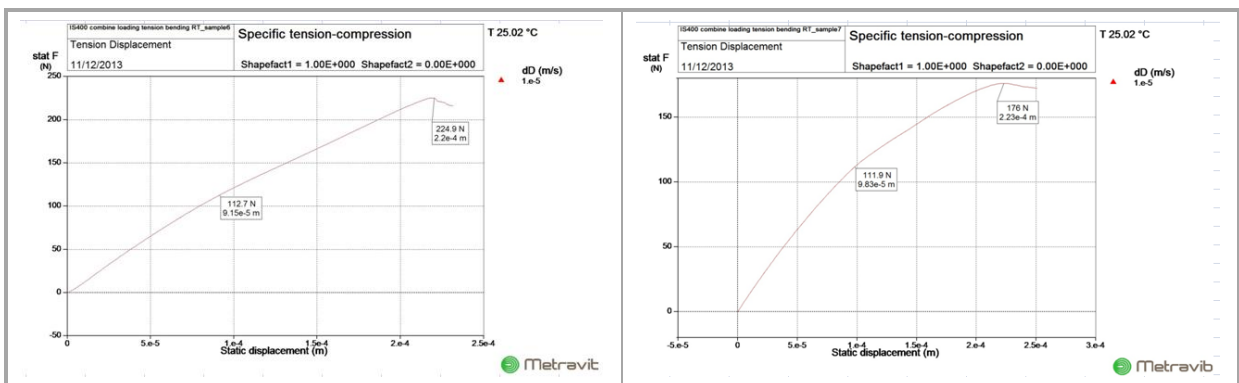


Figure 30: Force-displacement curves recording under combined loading up to failure

Additionally, load cases were run up to the yield strength, which was rated from the curves in Figure 30. Several of such force-displacement curves are shown in Figure 31.

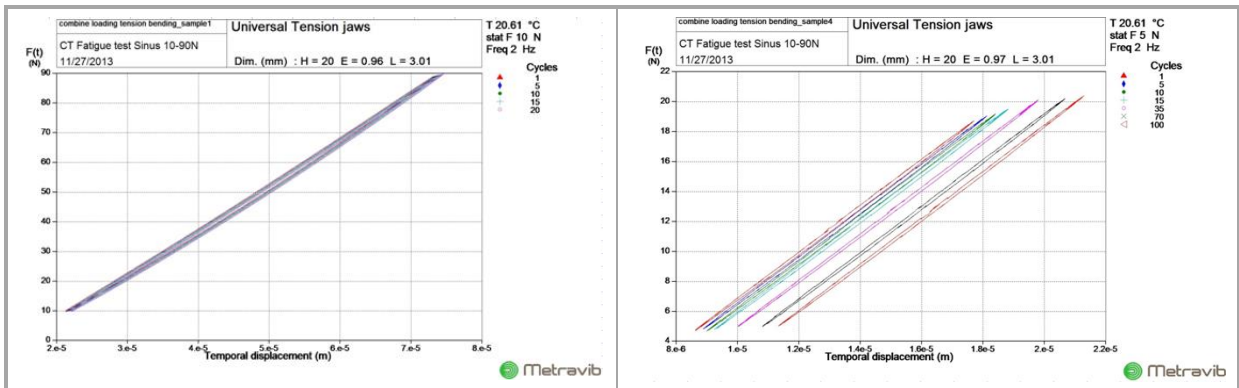


Figure 31: Force-displacement curves recording under combined loading up to estimated yield strength

Here, a cyclic loading resulted in a shifting of the force-displacement curve along the displacement axis. It seems likely, that no pure elastic deformation appears under these conditions. The experiments described above were performed using 5 plies specimen.

On the basis of [7] another experimental set-up was tested. In the previous experiments, the tensile force was applied eccentrically. In this case, the rotation is not fixed in a specific angle, but unlocked to allow an extra degree of freedom. Additional distance pieces were placed in the clamps to enable the eccentricity. The shape of the specimen remained the same as before. A force-displacement curve is shown in section 3.2.2 (Figure 36).

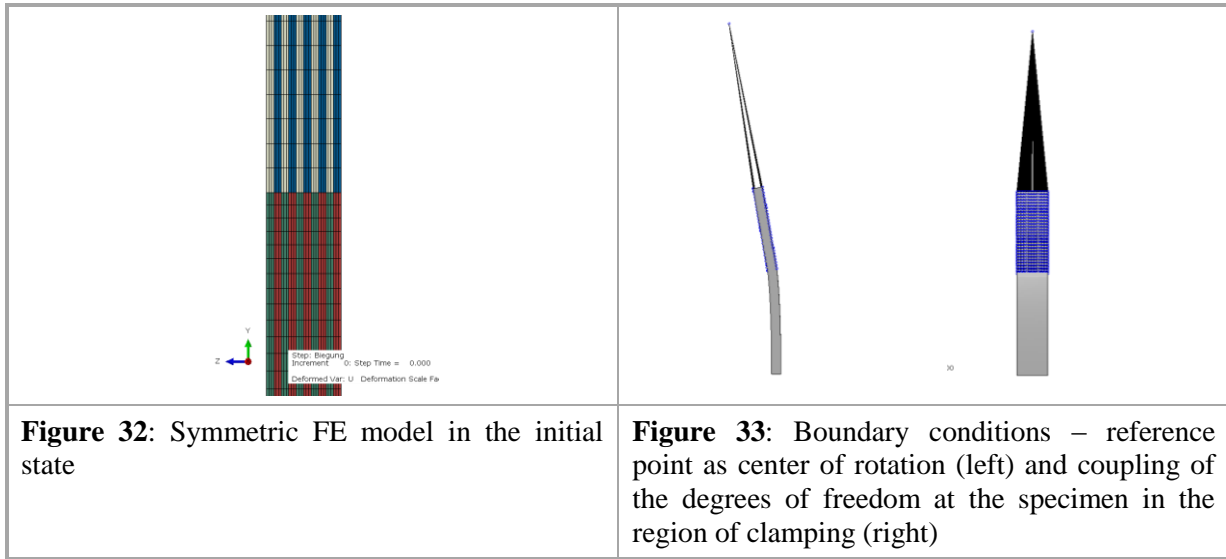
3.2 Numerical modeling – fracture and damage analysis

FRP laminates show a strong anisotropic material behavior due to the orientations of the fiber reinforcements. Because of these orientations different failure mechanisms occur and are more complex under multi-axial loading conditions.

3.2.1 FE model and material properties

The FE model (Figure 32) consists of 5 plies equivalent to the experiment. The applied boundary conditions are shown in Figure 33.

The dimensions used in the FE analysis are the same as used in the experiment.



The fiber orientation was implemented by the definition of the material orientation coordinate system by alternating order. An effective orthotropic material behavior of the fiber reinforced polymer composite was introduced in the FE simulations (Table 4). The different distances of the fiber bundles in the plane directions were realized by corresponding effective orthotropic material properties of the ply. The effective material properties were determined by tensile tests and corresponding FEA simulations in both in-plane directions as described in the WP2.

As suggested by Fraunhofer ENAS (ITD member), the damage and fracture threshold parameters were determined by evaluating the inelastic part of force vs. displacement behavior of the tensile tests under different fiber orientations. In Table 5 the resulting threshold parameters are composed for use within the utilized material model.

Layer	Material	Constitutive law	Young's modulus [GPa]	Poisson's ratio	Shear modulus [GPa]
<i>Longitudinal</i>	FRP composite	Elastic orthotropic incl. damage and failure for fiber-reinforced composites	$E_L = 21$ $E_T = 2.2$	$\nu_{12_LT} = 0.3$ $\nu_{23_LT} = 0.4$	$G_{12} = 8$ $G_{23} = 8$
<i>Transversal</i>	FRP composite	See <i>Longitudinal</i>	$E_L = 17$ $E_T = 2.2$	$\nu_{12_LT} = 0.3$ $\nu_{23_LT} = 0.4$	$G_{12} = 8$ $G_{23} = 8$

Table 4: Orthotropic material data applied in the FE model

Layer	Failure stress in L-direction [MPa]	Failure stress in T-direction [MPa]	Failure stress in 12-shear [MPa]
<i>Longitudinal</i>	$\sigma_{\text{tens}} = 420$ $\sigma_{\text{compr}} = 190$	$\sigma_{\text{tens}} = 330$ $\sigma_{\text{compr}} = 180$	$\sigma_{12_TL} = 40$
<i>Transversal</i>	$\sigma_{\text{tens}} = 310$ $\sigma_{\text{compr}} = 180$	$\sigma_{\text{tens}} = 380$ $\sigma_{\text{compr}} = 170$	$\sigma_{12_TL} = 40$

Table 5: Orthotropic damage initiation properties applied in the FE model [1]

3.2.2 Simulation results

The simulation results of the failure were in a qualitatively good agreement with the experiment. As experimentally observed the damage initiation occurs at the edges of the clamps. The progress of damage in the fiber (variable SDV1) and matrix (SDV2) are represented in table 5. The development of the maximum principle stress was added for comparison to the stress state. The model of damage chosen in this investigation describes the failure due to exceeding of the critical stress value (compression/tension) perpendicular or parallel to the fiber direction. The critical regions can be recognized by the maximal mean stresses.

The simulation was performed up to tensile load of 20 μm . However, the quantitative relation between the force and displacement does not fully agree between experiment and simulation. In the simulation the damage occurs earlier than in the experiment. The tables below (Table 6-8) illustrate the chronology of the failure appearance in the different constituents of the composite (Table 6-7 fiber damage compared to reference and Table 8 fiber and matrix damage compared to reference, matrix damage occurred first after tensile step time of 1.9 s). Where “maximum principle stress” is the stress value used as reference, “SDV1 fiber damage” is the variable state of damage illustrating the failure in the fibers and “SDV2 matrix damage” is the variable state of damage in the matrix material. A damage variable value of “0” means no damage exists and a value of “1” means the element is completely damaged. The picture are arranged on the same time scale.

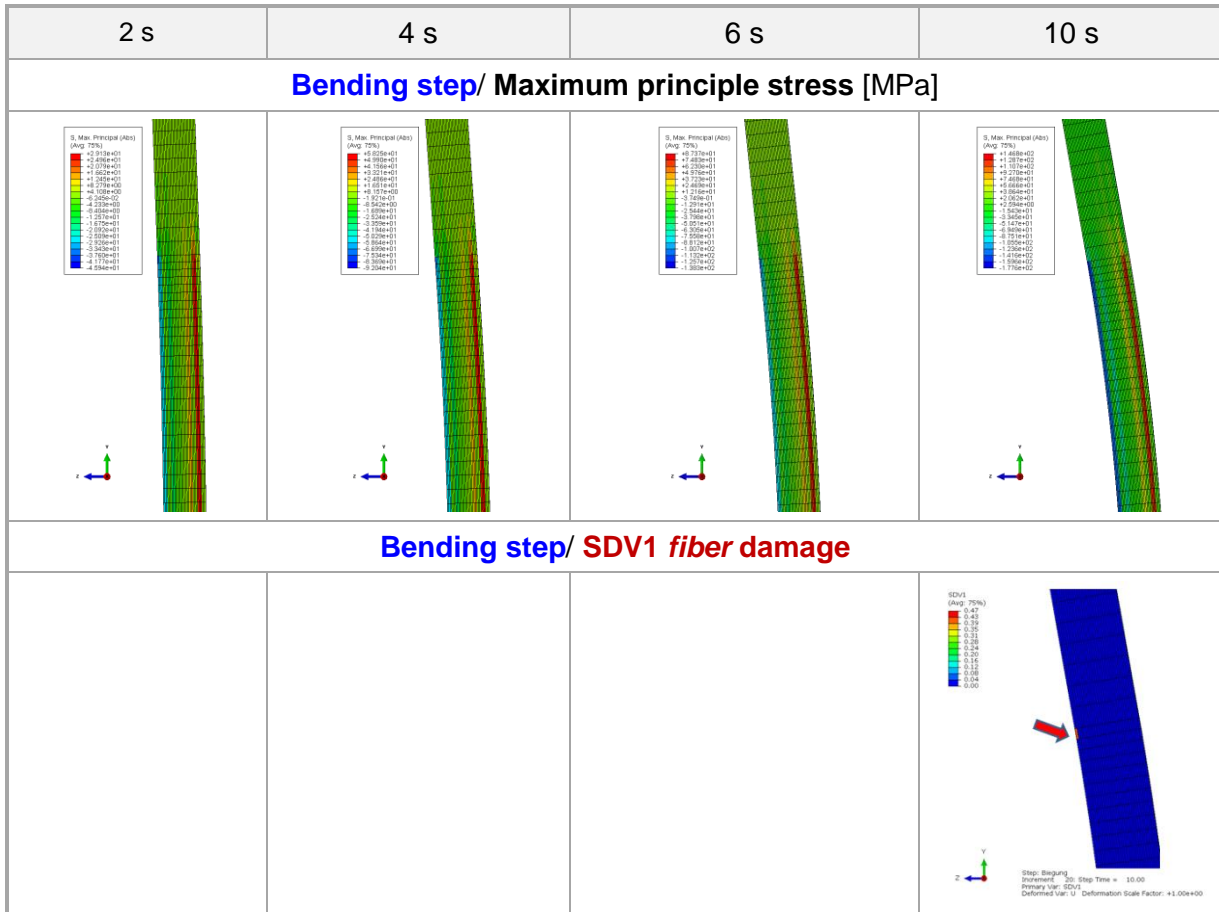
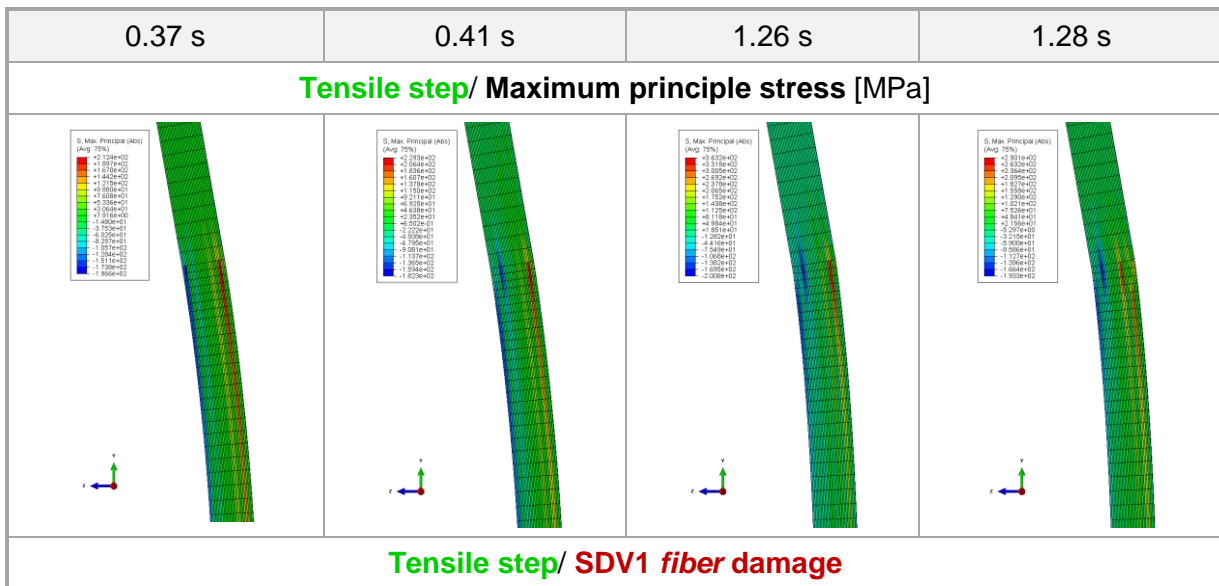


Table 6: FE simulation results – progress of fiber damage in comparison with the v. MISES stress for bending step time up to 10s



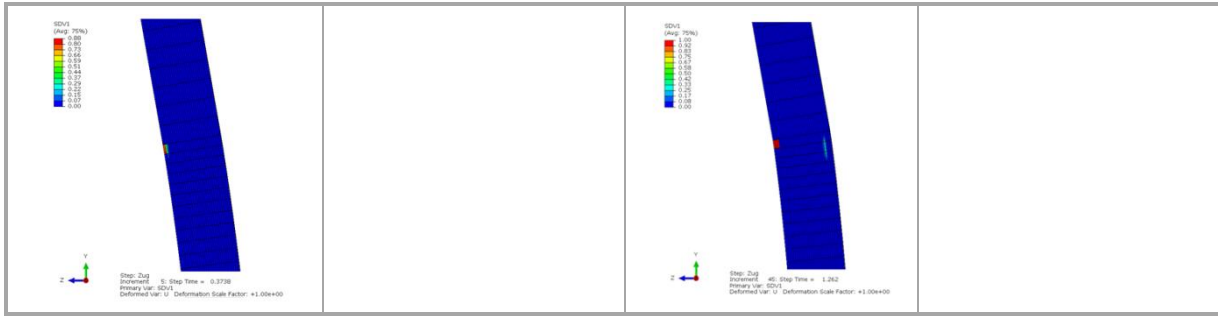


Table 7: FE simulation results – progress of fiber damage in comparison with the v. MISES stress for tensile step time up to 1.26 s

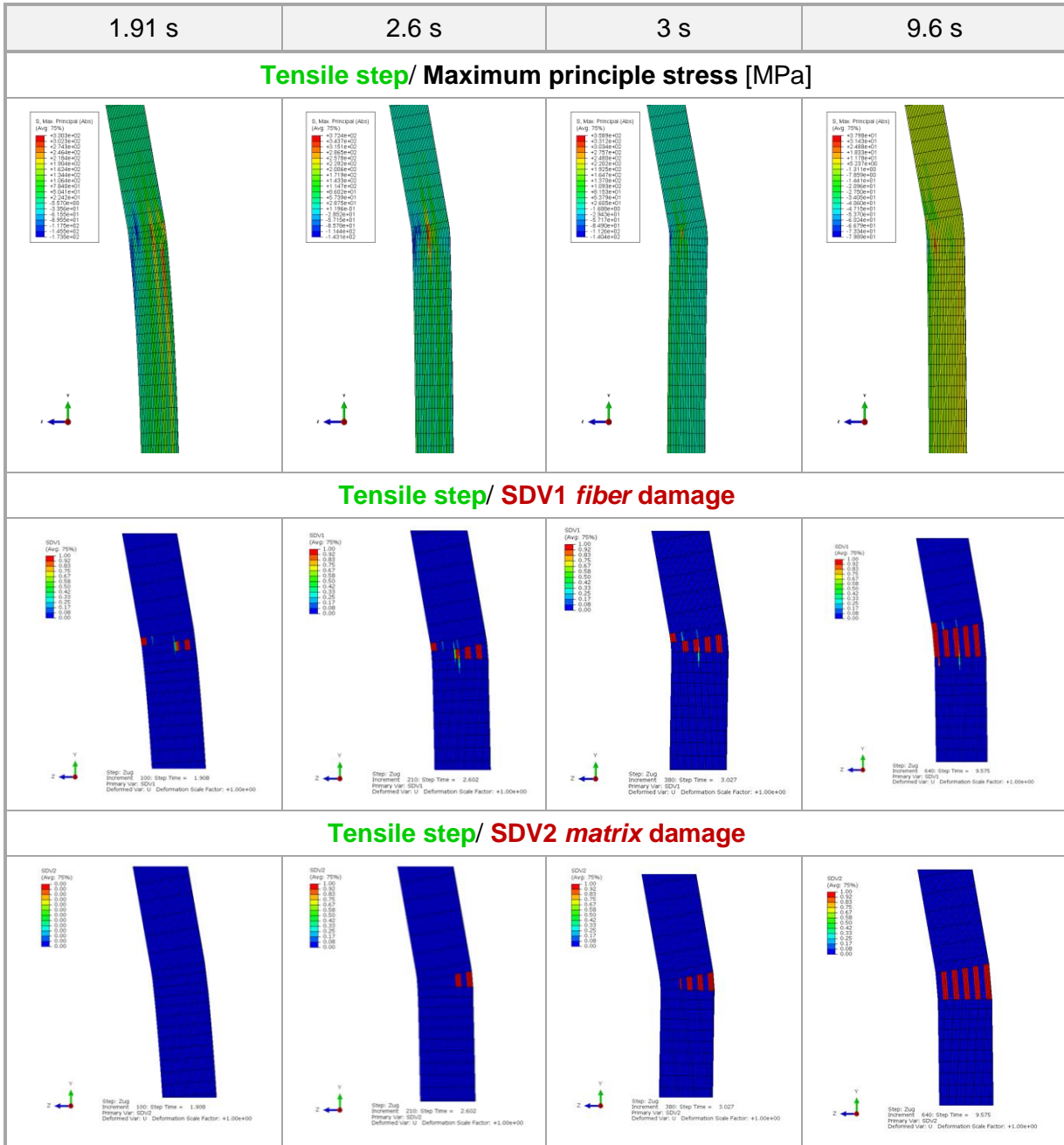


Table 8: FE simulation results – progress of fiber and matrix damage in comparison with the v. MISES stress for tensile step time up to 9.6 s

After evaluation of the measurements and the appropriate simulations the experimental set-up was modified and corresponds more with [7] as described in section 3.1. The bending angle is no longer fixed and distance pieces realize the eccentricity of the beam to the tensile axis. Now, the bending moment is a result of the tension load at which the beam bending approximates the value of the implemented eccentricity (see Figure 35), in this case 0.5 and 1 mm. After starting the tensile load the bending stress was dominant. Figure 34 illustrates the stress/strain behavior at the compression and the tension side. It is obviously that advanced loading resulted in tensile stress at both sides. The bigger the eccentricity the larger the bending strain values at the compression and tension side. In the FE simulation the loading was applied displacement controlled up to 70 μm .

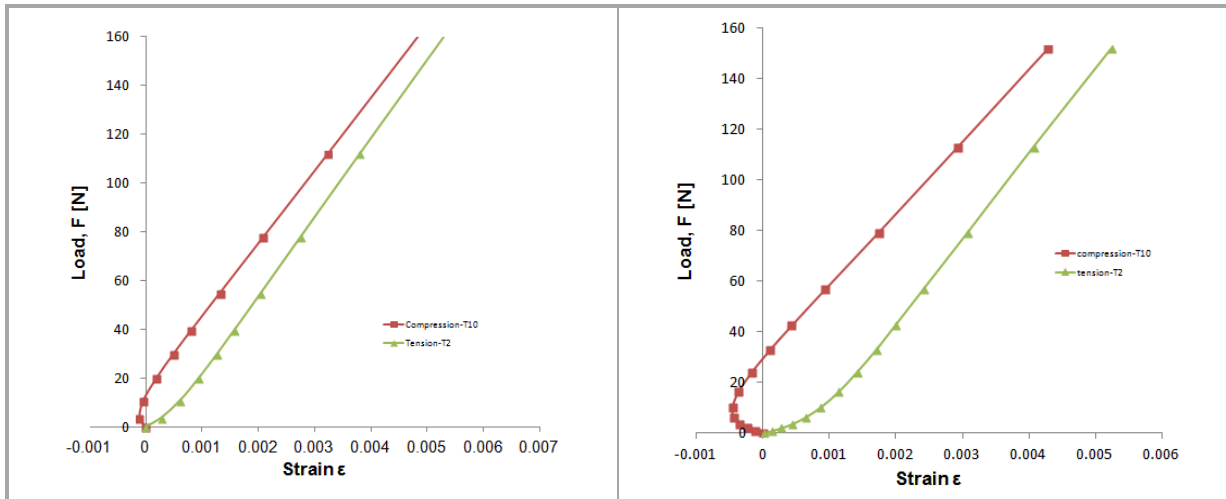


Figure 34: Force-strain curve for combined bending and tension load obtained from FE simulation (left - eccentricity 0.5 mm, right - eccentricity 1 mm)

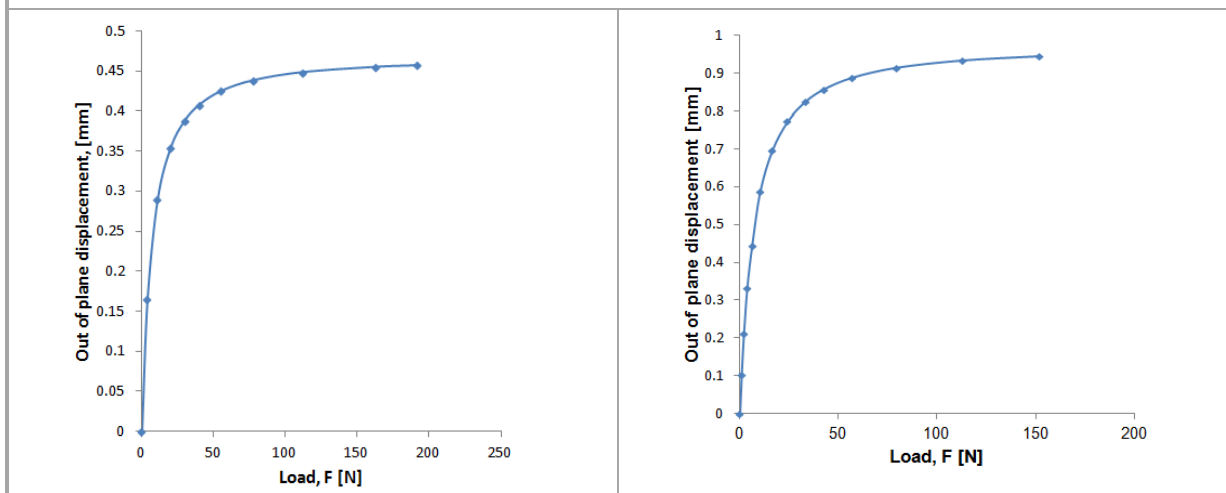


Figure 35: Out of plane displacement at the specimen center as a function of force obtained from FE simulation (left - eccentricity 0.5 mm, right - eccentricity 1 mm)

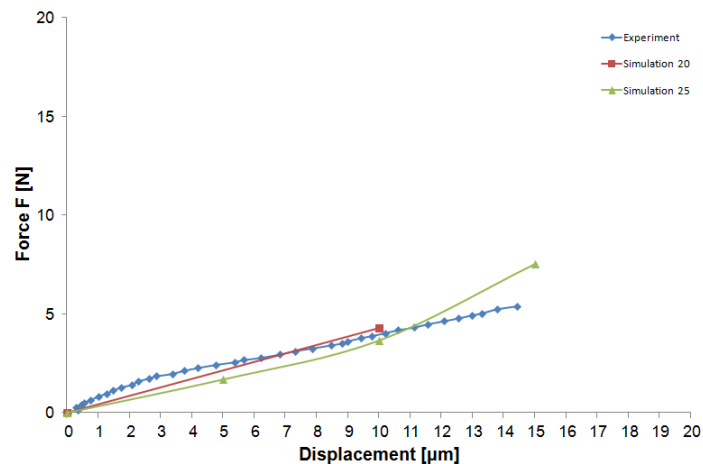


Figure 36: Comparison of the experimental (blue) and simulated (red and green) force - displacement curves with two different sample lengths (20 mm and 25 mm)

Figure 36 shows the comparison of the force - displacement curves obtained by experiment and simulation. In this region of loading a good agreement between experimental and simulation results was found. The influence of the sample length is relative low for the used specimens.

The tendency of the green curve seems to have a noticeable stiffer behavior than the experimental set-ups. This can be due to the use of an infinitely stiff sample holder in the simulation where in the experiment the sample holder is loose and allow some displacement not related to the sample.

3.3 Conclusions

WP3 addresses the expansion of the methodology [3] to complex loading conditions combining several contributions like tensile, torsion and shear. Here, the multi-axial load situation in the FRP is realized by combined tension-bending loading. WP3 compile all experience gathered through the project and some additional results (fracture criterion) obtained in the CfP MIFACRIT to combine them in a global model taking into account the failure criterion to predict the composite behavior under combined loading. A sample holder for combined tension and bending load was developed and experiments were carried out according to the working plan. Simulation model has been generated respective to the experimental settings.

Simulation results on the first approach show good qualitative agreement to the experiment but are quantitatively slightly different. The fiber break first in the model as in the observation the matrix seems to fail first. On the second set of simulation, on the combine loading with free rotation axes, the simulation results are much stiffer that what was measured, this could be due to experimental difficulties bond to the compliance calibration of the sample holder.

Finally the procedure of capturing by simulation elastic properties as well as failure/damage properties under combine loading of the multiply composites has been achieved.

All these elements were the prerequisite to the “Multi-axiality expansion” which is successfully finished in the framework of WP 3.

References

- [1] SIMULIA (ABAQUS) Manuals (V. 6.11), Dassault Systemes Simula Corp., Providence, RI, USA, 2011
- [2] Miyano, Y., Nakada, M., and Sekine, N. 2004. "Accelerated testing for long-term durability of GFRP laminates for marine use". *Composites Part B: Engineering* 35, 6-8 (2004/9), 497–502.
- [3] Miyano, Y., Nakada, M., and Nishigaki, K. 2006. "Prediction of long-term fatigue life of quasi-isotropic CFRP laminates for aircraft use". *The Third International Conference on Fatigue of Composites. International Journal of Fatigue* 28, 10 (2006/10), 1217–1225.
- [4] MatWeb: E-Glass Fiber, Generic. In: www.matweb.com. Stand: 14.05.2012. URL: <http://www.matweb.com/search/DataSheet.aspx?MatGUID=d9c18047c49147a2a7c0b0bb1743e812&ckck=1>(letzer Abruf: 14.05.2012)
- [5] J. Rösler, H. Harders, M. Bäker; *Mechanisches Verhalten der Werkstoffe*; Teubner Verlag; 1. Auflage, Juni 2003
- [6] ANSYSTM Multiphysics, version 14.5, User's manual, Ansys Inc.
- [7] Khoshbakht, M., Chowdhury, S.J., Seif, M.A., Khashaba, U.A., "Failure of woven composites under combined tension-bending loading", *Composite Structures* 90 (2009) 279–286

Potential impact and main dissemination activities and exploitation results

In convergence with the objectives of the Clean Sky Joint Undertaking JTI-CS-2010-3-ECO-01-007 the project brought together experts in the field of materials testing and property evaluation with the aim of delivering a methodology for evaluating of the long-term fatigue life of CFRP structures.

Materials design and testing has been recognized as a key requirement by airframe manufacturers including all major players. According to the ECO-Design ITD the minimization of the consumption of non-renewable fossilized materials goes along with the need for weight reduction of aircraft structures.

Development of highly effective and weight saving composite materials for civil aircraft was identified as a key enabler in meeting the goals of the ACARE 2020 challenge.

The understanding of the long-term behavior of CFRP structures is a key for the implementation of new materials in the aircraft industry. It is necessary for a world-class capability in this field to exist in Europe. Consequently, the competitiveness of the knowledge-intensive European SMEs will be increased.

FATIMA project supports that goal by:

- Improving the predictive capabilities of fatigue testing and material evaluation
- Having a methodology available for dedicated design of CFRP stacks using a powerful tool box

By the dissemination action and conference-papers the methodology was published to the scientific and industrial community. The exploitation will be driven by the project partners. Relevant customers for the methodology were identified and contacted to realize a shorter time-to-market and competitiveness of newly developed CFRP systems.

Results of the project serve as the basis for future analysis services. The strength of the method is established by a combination of experimental and simulative methods which forms the toolbox for fatigue analysis.

Address of project public website and relevant contact details

During the project a website was not provided

For dissemination of the project main results will be published under website of AMIC

<http://www.amic-berlin.de>

including links to other partners.

Partner 1:

Dr.-Ing. Jürgen Keller

AMIC Angewandte Micro-Messtechnik GmbH

Volmerstraße 9B

D-12489 Berlin

phone: +49 30 6392 2540

fax: +49 30 6392 2544

email: Juergen.Keller@amic-berlin.de

url: www.amic-berlin.de

Partner 2:

Dipl.-Ing. Bettina Seiler

Chemnitzer Werkstoffmechanik GmbH

Technologie-Campus 1

D-09126 Chemnitz

Germany

phone: +49 371 5347 960

fax: +49-371 5347 961

email: Seiler@cwm-chemnitz.de

url: www.cwm-chemnitz.de

Partner 3:

Dr. Thomas Winkler

Berliner Nanotest und Design GmbH

Volmerstraße 9B

D-12489 Berlin

phone: +49 30 6392 3880

fax: +49 30 6392 3881

email: Thomas.Winkler@nanotest.org

url: www.nanotest.org